EXPERIMENTAL VALIDATION OF CONSTITUTIVE RELATIONS INCLUDING DUCTILE FRACTURE DAMAGE

G. Rousselier*, J. C. Devaux and G. Mottet****

**Electricité de France, Département Etude des Matériaux, Les Renardières, 77250 Moret-sur-Loing, France*

***Framatome, Service Calcul de la Division des Fabrications, Usine de Chalon-sur-Saône, 71380 Saint-Marcel, France*

ABSTRACT

Some difficulties arise in the risk analysis of initiation and growth of cracks by ductile tearing based on the resistance curve concept (J-Δa). An alternative method consists in modelling the damage occurring at the crack tip by means of constitutive relations impaired by the ductile fracture damage.

An experimental programme has been completed in order to validate this method for A 508 cl. 3 steel. Firstly the predictions of the model have been compared with void growth measurements. Secondly the constitutive relations have been introduced in a finite element programme (TITUS) and the simulation of tensile tests has been performed.

The numerical simulation of notched axisymmetric specimen rupture proved successful and the technique presented here can be considered as an engineering tool to predict crack initiation, stable crack growth and final instability. The simulation of cracked specimens is in the making in order to complete the calibration and the validation of this method.

KEYWORDS

Ductile fracture, constitutive relations, damage, void nucleation, void growth, material instability, finite element, numerical analysis.

INTRODUCTION

The risk analysis of initiation and growth of cracks by ductile tearing in PWR components is currently based on the resistance curve concept. Two difficulties arise :

- the resistance curve J-Δa is not an intrinsic property of materials (Marandet and co-workers, 1982) ;
- the J-integral calculation is sometimes problematic (3D and thermal loads).

Our method consists, within the field of continuum mechanics, in modelling the damage occurring at crack tip ; the restrictions quoted above are no longer effective. The constitutive relations which have been developed take into account the void growth occurring during ductile fracture damage ; their detailed formulation is given by Rousselier (1978, 1981) and we will merely recall its main features hereafter.

The validation of the model is based on the void growth measurements performed by Mudry (Beremin, 1981) and on the numerical simulation of experiments on circumferentially notched tensile specimens (Rousselier, Phan Ngoc and Mottet, 1983). The numerical simulation is performed by running a finite element programme (TITUS) using an updated lagrangian formulation and involving the void growth.

CONSTITUTIVE RELATIONS

The plastic potential contains an extra term related to the damage and depending on the hydrostatic stress $\sigma_m = \sigma_{ll}/3$:

$$F(\sigma/\rho, p, \beta) = \sigma_{eq}/\rho - R(p) + B(\beta).f(\sigma_m/\rho) \tag{1}$$

In equation (1) σ_{eq} is the equivalent von Mises stress, ρ the density ($\rho(0) = 1$), p the cumulated plastic strain ($\dot{p} = \dot{\varepsilon}^{p}_{eq}$), and β the damage variable ; β is a scalar since the damage is assumed to be isotropic.

The normality rule is assumed for the plastic strain rate <u>and</u> the internal variable rate $\dot{\beta}$, as proposed by Nguyen (1973) :

$$\dot{\varepsilon}^{p}_{ij} = \dot{p}\ \partial F/\partial(\sigma_{ij}/\rho) \tag{2}$$

$$\dot{\beta} = \dot{p}\ \partial F/\partial B = \dot{p} f(\sigma_m/\rho) \tag{3}$$

The combination of equations (2) and (3) into the mass conservation law $\dot{\rho} + \rho\dot{\varepsilon}^{p}_{ll} = 0$, with $\dot{\rho} = \dot{\beta} d\rho(\beta)/d\beta$, gives :

$$f'(\sigma_m/\rho)/f(\sigma_m/\rho) = -d\rho(\beta)/\rho(\beta)B(\beta)d\beta \tag{4}$$

Therefore the two sides of equation (4) are constant of dimension $1/\sigma$, say $1/\sigma_1$. The integration of the left-hand side gives the <u>exponential dependence on hydrostatic stress</u> σ_m (D is the constant of integration):

$$f(\sigma_m/\rho) = D\exp(\sigma_m/\rho\sigma_1) \tag{5}$$

This result is in agreement with both theoretical studies (McClintock, 1968 ; Rice and Tracey, 1969 ; Gurson, 1977) and experimental results (Hancock and Brown, 1983 ; Beremin, 1981).

VOID NUCLEATION AND GROWTH

Since the initiation of void growth does not coincide with the beginning of plastic deformation, the void nucleation criterion proposed by Beremin (1981) is used :

$$\Sigma_1 + k(\sigma_{eq} - \sigma_0) = \sigma_c \tag{6}$$

Σ_1 is the maximum principal stress, σ_0 the yield stress of the material, k and σ_c are constants. When the criterion (6) is not met, equation (3) is replaced by $\beta = \dot{\beta} = 0$.

As for the void growth, let us consider spherical voids of radius R in an incompressible matrix. The functions $\rho(\beta)$ and $B(\beta)$, related by equation (4), are assumed to be :

$$\rho(\beta) = 1/(1 - f_0 + f_0\exp\beta) \qquad B(\beta) = \sigma_1 f_0 \exp(\beta)\rho(\beta) \tag{7}$$

where f_0 is the initial void volume fraction. This choice yields the simple relation $\dot{\beta} = 3\dot{R}/R$, hence :

$$\dot{R}/R = (D/3)\ \dot{\varepsilon}^{p}_{eq} \exp(\sigma_m/\rho\sigma_1) \tag{8}$$

If the variation of ρ is neglected, and if $D/3 = 0.283$ and $\sigma_1 = 2\sigma_0/3$, equation (8) is identical to the high triaxiality approximation of Rice and Tracey (1969) for a single void in a non-hardening matrix.

The relations (7) will be retained hereafter. Still equation (8) has to be experimentally validated, and the constants D and σ_1 have to be determined for a given strain-hardening material. For that purpose we used the measurements of void growth performed by Mudry (Beremin, 1981) on circumferentially notched tensile specimens taken from nozzle dropouts of PWR nuclear vessels.

The stresses and strains at a given location in the minimum section are known through finite element analyses of the specimens. Equation (8), with $\rho = 1$, is integrated from ε_d to the final strain ε_{eq}, where ε_d is the decohesion strain resulting from the criterion (6) ; for A 508 cl.3 steel the constants of equation (6) are (Beremin, 1981 b) :

- longitudinal direction $k = 1.6$ $\sigma_c = 1120$ MPa (9)

- short transverse direction $k = 0.6$ $\sigma_c = 810$ MPa (10)

Actually the integration of equation (8) is approximate : as σ_m/σ_{eq} is almost constant during the loading of the specimens, it is assumed that $\sigma_m = \text{constant} \times \varepsilon^n$, where n is the best fit hardening exponent of the material between ε_d and ε_{eq}. The resulting form is :

$$\ln[\ln(R/R_0)/\omega\varepsilon_{eq}] = \ln(D/3) + (1/\sigma_1)\sigma_m \tag{11}$$

The decohesion strain and the stress history are taken into account through the corrective factor ω[1].

The experimental points are given in Fig. 8. A linear regression analysis gives the constants $\ln(D/3)$ and $1/\sigma_1$ (a few iterations are required, as ω depends on σ_1) :

- longitudinal direction $\sigma_1 = 390$ MPa $D = 2.02$ (12)

- longitudinal + short transverse directions $\sigma_1 = 386$ MPa $D = 1.87$ (13)

---

[1] Let $a = \sigma_m/\sigma_1$, $b = \varepsilon_d/\varepsilon_{eq}$, $N = (n+1)/n$. Then :

$$\omega = 1 - \frac{a}{N} + \frac{a^2}{N(N+1)} - \frac{a^3}{N(N+1)(N+2)} + \cdots - b(\exp a)^{b^n - 1}\left[1 - \frac{b^n a}{N} + \frac{(b^n a)^2}{N(N+1)} - \cdots\right]$$

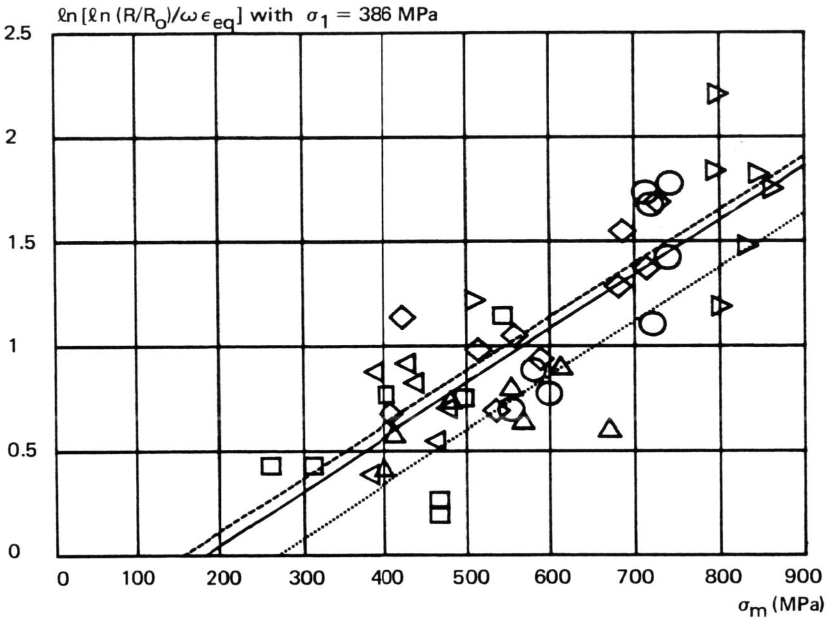

Fig. 8 – Measured void growth in the longitudinal (L : ▷ ◇ □) and short transverse (ST : ○ △ ◁) directions. Regression lines L (----- , σ_1 = 390 MPa, D = 2.02), L + ST (——, σ_1 = 386 MPa, D = 1.87) and line (············ , σ_1 = 385 MPa, D = 1.5).

Considering the large scatter of the measured void growths, the difference between the two directions is not significant. Equation (8) gives a good description of the void growth, and the constants D and σ_1 have been roughly estimated for A 508 cl. 3 steel with a volume fraction of inclusions $f_o = 10^{-4}$ to 10^{-3} (for $f_o < 10^{-3}$ the void growth measurements performed by Marini (Devaux and co-workers, 1982) and Sun Yao Qing and co-workers (1983) suggest a dependence of D on f_o).

NUMERICAL SIMULATION OF DUCTILE FRACTURE INITIATION

Two circumferentially notched tensile specimens (notch radius 2 mm) have been taken in the longitudinal direction from a nozzle dropout of a PWR nuclear vessel. The experiments have been conducted at 100°C.

The load-displacement curves (in terms of diameter contraction) of the notched specimens are plotted in Fig. 1 ; in these specimens, the ductile fracture initiates in the center and is accompanied by a marked change in the slope of the load-displacement curve as shown by

interrupted tests (Rousselier, 1978). The mean strain $\varepsilon = 2\ \ln(D_o/D)$ in the minimum section of the specimens reaches 35 % and 36.4 % at ductile fracture initiation and the ultimate fracture comes just after the initiation.

The true stress-strain curve of the material has been measured on unnotched specimens for strains up to 10 % ; the measured hardening exponent is n = 0.1 and this value has been retained for larger strains : $\sigma = \text{constant} \times \varepsilon^n$. The volume fraction of inclusions used in the model is deduced from the chemical composition and from the quantitative analysis of the inclusions :

$$f_o = 2.5 \times 10^{-4} \times \sqrt{d_T d_{ST}} / d_L = 1.6 \times 10^{-4} \qquad (14)$$

The corrective factor takes into account the mean dimensions of the inclusions : d_T = 8.3 µm, d_{ST} = 6.9 µm, d_L = 11.5 µm ; it is based on the assumption that the dimensions in the plane of fracture only are significant for the void growth (Mudry, 1982). Anyway the correction is small.

The nucleation criterion (6) is used with k = 1.6 and σ_c = 1120 MPa. In the damage equation D = 1.5 is retained and three successive calculations have been carried out with σ_1 = 300, 380 and 400 MPa.

The calculations have been carried out with the eight-node element mesh plotted in Fig. 2 ; a reduced integration scheme (2 x 2) has been adopted in order to avoid the violation of incompressibility conditions resulting from the (3 x 3) integration. The large changes in geometry are taken into account by modifying the coordinates at each load step ; the density changes are also modelled in the computation of the stiffness matrix : $\dot{\sigma} = (\rho L)(\dot{\varepsilon} - \dot{\varepsilon}^P)$, where L is the usual elastic moduli tensor.

The calculated load-displacement curve is plotted in Fig. 3, in which the experimental results have been indicated : the numerical simulation proves quite satisfactory. The relation between the uniform displacement Uy applied at the end of the specimen and the diametral contraction is plotted in Fig. 4. The evolution of the longitudinal stress σ_{yy} and of the damage parameter is plotted in Fig. 5 and 6 for the first integration point of elements close to the center. The mechanical state (stresses, strains, damage) is rather homogeneous in this region and the damage zone stretches out in the minimum section (figure 7).

The noticeable drop in the longitudinal stress observed in Fig. 5 corresponds to the last phase of void growth : the void coalescence results in the initiation of a crack at the center of the specimen. The stable crack growth simulation (which in our case could be rendered without releasing nodes) has not been attempted in the present calculation.

Let d_c be the critical displacement at crack initiation ; the estimation of d_c in function of the constant σ_1 is plotted in Fig. 9, in which the experimental results are indicated. The resulting constants are:

$$\sigma_1 = 385 \text{ MPa} \qquad D = 1.5 \qquad (15)$$

This result is in good agreement with the constants (12) and (13) resulting from the void growth measurements. The corresponding line is plotted in Fig. 8. A better agreement is not expected, for the following reasons :

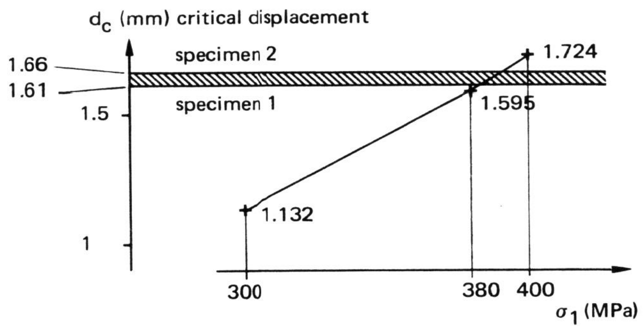

Fig. 9 – Comparison of experimental and numerical displacements at the initiation of a ductile fracture crack. Calibration of the constant σ_1 (with D = 1.5).

- the large scatter in void growth measurements,
- the limited interval of σ_m investigated (σ_m < 860 MPa),
- the approximate analysis of stress and strain history.

Thus it is demonstrated that constitutive relations, by means of which ductile fracture occurs by strain localization, can give quite realistic critical strains. Several authors (e.g. Yamamoto, 1978) questionned this possibility and had to introduce some initial inhomogeneity in the distribution of porosity. This complication is obviously not necessary.

CONCLUSIONS

Elastic-plastic constitutive relations including ductile fracture damage have been proposed. With these relations ductile fracture occurs by localization of deformation in the most damaged part of the structure.

The model has been validated and calibrated both at the microscopic (void growth measurements) and macroscopic levels (initiation of fracture in the center of a tensile specimen).

The ability of the method to model crack initiation and stable crack growth in a precracked specimen has already been demonstrated (Rousselier, 1981, 1983). A complete validation and calibration of the method is in progress on circumferentially cracked tensile specimens. The method, implemented in a finite element programme (TITUS), will then be available in order to assess the ductile tearing risk in PWR components.

ACKNOWLEDGMENTS

The authors are grateful to Dr F. Mudry for the communication of the detailed results of his void growth measurements. The numerical computations have been carried out by FRAMATOME.

REFERENCES

Beremin, F.M.[1] (1981 a). Study of fracture criteria for ductile rupture of A 508 steel. Advances in Fracture Research, (ICF5), D. François editor, Pergamon Press, 2, 809-816.

Beremin, F.M. (1981 b). Experimental and numerical study of the different stages in ductile rupture : application to crack initiation and stable crack growth. Three dimensional constitutive relations and ductile fracture, S. Nemat-Nasser editor, North-Holland, 185-205.

Devaux, J.C., B. Marini, F. Mudry and A. Pineau (1982). Etude de l'amorçage et de la propagation stable des fissures en milieu tridimensionnel utilisant un critère physique de rupture ductile. Colloque Méthodes de Calcul, DGRST, March 3, 1982, Antibes, France.

Gurson, A.L. (1977). Continuum theory of ductile rupture by void nucleation and growth : Part I - Yield criteria and flow rules for porous ductile media. J. Engng. Mat. Tech., 99, 2-15.

Hancock, J.W., and D.K. Brown (1983). On the role of strain and stress state in ductile failure. J. Mech. Phys. Solids, 31, 1-24.

McClintock, F.A. (1968). A criterion for ductile fracture by the growth of holes, J. Appl. Mech., 35, 363-371.

Marandet B., G. Phelippeau, P. de Roo and G. Rousselier (1982). Effect of specimen dimensions on J_{IC} at initiation of crack growth by ductile tearing. 15th ASTM Symposium on Fracture Mechanics, July 7-9, 1982, College Park, Maryland, USA.

Mudry, F. (1982). Etude de la rupture ductile et de la rupture par clivage d'aciers faiblement alliés. Thèse d'Etat, Université de Technologie de Compiègne.

Nguyen, Q.S. (1973). Contribution à la théorie macroscopique de l'élastoplasticité avec écrouissage. Thèse d'Etat, Université de Paris VI.

Rice, J.R., and D.M. Tracey (1969). On the ductile enlargement of voids in triaxial stress fields. J. Mech. Phys. Solids, 17, 201-217.

Rousselier, G. (1978). An experimental and analytical study of ductile fracture and stable crack growth. Specialists Meeting on Elastic-plastic Fracture Mechanics, May 22-24, 1978, Daresbury, UK, OECD-NEA-CNSI report 32, Vol. 2, Paper n° 14.

Rousselier, G. (1981). Finite deformation constitutive relations including ductile fracture damage. Three dimensional constitutive relation and ductile fracture, S. Nemat-Nasser editor, North-Holland, 331-355.

Rousselier, G., K. Phan Ngoc and G. Mottet (1983). Elastic-plastic constitutive relations including ductile fracture damage. 7th International Conference on Structural Mechanics in Reactor Technology, Paper G/F n°1/3.

Sun Yao Qing, J.M. Devaux, G. Touzot and D. François (1983). Mécanique de la rupture ductile dans la fonte à graphite sphéroïdal ferritique. Mémoires Scientifiques de la Revue de Métallurgie, April 1983, 183-195.

Yamamoto, H. (1978). Conditions for shear localization in the ductile fracture of void-containing materials. Int. J. Fracture, 14, 347-365.

[1] Beremin F.M. is a research group including Y. d'Escatha, J.C. Devaux, J.C. Lautridou, F. Ledermann, F. Mudry and A. Pineau.

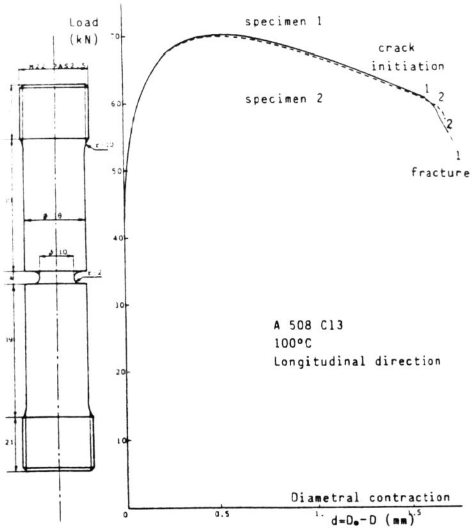

Fig. 1 - Geometry and load displacement curves of the notched axisymetric tensile specimens (diameter D_o = 10mm)

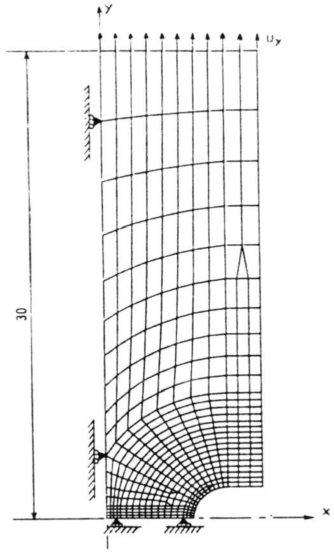

Fig. 2 - Finite element mesh

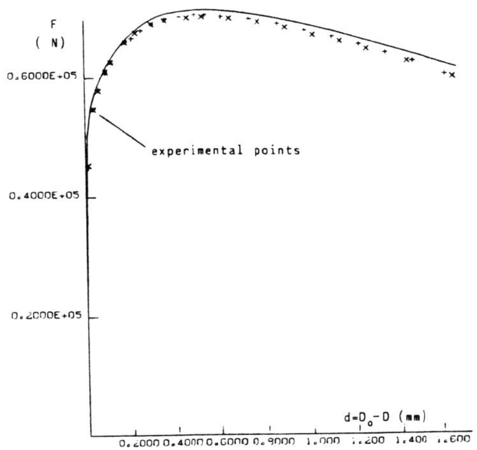

Fig. 3 - Calculated load-displacement curve

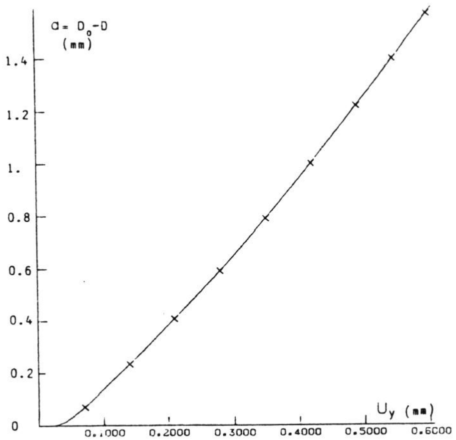

Fig. 4 - Diametral contraction versus displacement imposed at the end of the mesh

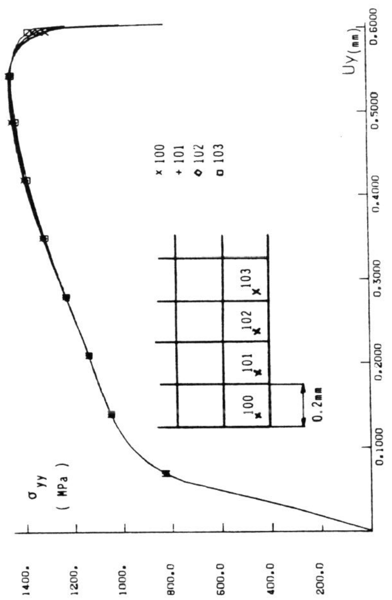

Fig. 5 - Longitudinal stress in the center of the specimen (σ_1 = 380MPa)

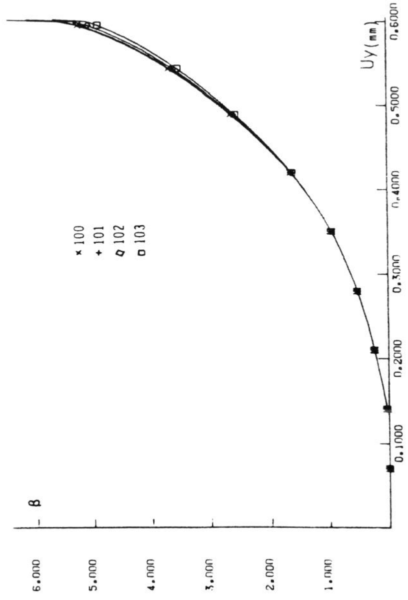

Fig. 6 - Damage parameter β in the center of the specimen (σ_1 = 380 MPa)

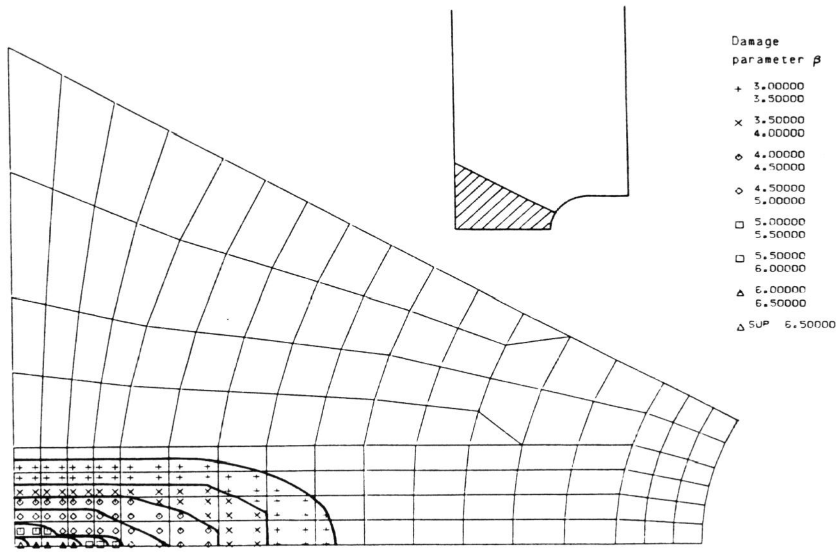

Fig. 7 - Damaged zones in the center of the specimen at ductile fracture initiation